

Quantitative vs. qualitative evaluation of static stress computed tomography perfusion to detect haemodynamically significant coronary artery disease

Gianluca Pontone^{1*}, Daniele Andreini^{1,2}, Andrea I. Guaricci³, Marco Guglielmo¹, Andrea Baggiano¹, Giuseppe Muscogiuri¹, Laura Fusini¹, Margherita Soldi¹, Fabio Fazzari⁴, Claudio Berzovini⁵, Annalisa Pasquini⁶, Paolo Ciancarella⁷, Saima Mushtaq¹, Edoardo Conte¹, Giuseppe Calligaris¹, Stefano De Martini¹, Cristina Ferrari¹, Stefano Galli¹, Luca Grancini¹, Paolo Ravagnani¹, Giovanni Teruzzi¹, Daniela Trabattoni¹, Franco Fabbicocchi¹, Alessandro Lualdi¹, Piero Montorsi^{1,2}, Mark G. Rabbat^{8,9}, Antonio L. Bartorelli^{1,10}, and Mauro Pepi¹

¹Centro Cardiologico Monzino, IRCCS, Via C. Parea 4, 20138 Milan, Italy; ²Department of Cardiovascular Sciences and Community Health, University of Milan, Via C. Parea 4, 20138 Milan, Italy; ³Department of Emergency and Organ Transplantation, Institute of Cardiovascular Disease, University Hospital "Policlinico" of Bari, Piazza Giulio Cesare 11, 70124 Bari, Italy; ⁴Department of Cardiology, University Hospital P. Giaccone, Via del Vespro 129, 90127 Palermo, Italy; ⁵Department of Surgical Sciences, Radiology Institute, University of Turin, Corso Bramante, 88, 10126 Torino, Italy; ⁶Dipartimento di Cardiologia, "La Sapienza" University of Rome, Viale del Policlinico, 155, 00161 Roma, Italy; ⁷Department of Radiology, Università degli Studi di Roma Tor Vergata, Viale Oxford, 81, 00133 Roma, Italy; ⁸Loyola University of Chicago, 1032 W Sheridan Rd, Chicago, 60660 IL, USA; ⁹Edward Hines Jr. VA Hospital, 5000 5th Ave, Hines, 60141 IL, USA; and ¹⁰Department of Biomedical and Clinical Sciences "Luigi Sacco", University of Milan, Via C. Parea 4, 20138 Milan, Italy

Received 21 January 2018; editorial decision 9 July 2018; accepted 21 July 2018

Aims

To compare the diagnostic accuracy of stress computed tomography myocardial perfusion (CTP) for the detection of significant coronary artery disease with visual approach vs. quantitative analysis with transmural perfusion ratio (TPR) in consecutive symptomatic patients scheduled for invasive coronary angiography (ICA) plus invasive fractional flow reserve (FFR).

Methods and results

Eighty-eight consecutive symptomatic patients underwent rest coronary computed tomography angiography (cCTA) followed by static stress-CTP. Diagnostic accuracy of cCTA + stress-CTP with visual evaluation and with TPR measurement was calculated and compared with ICA and invasive FFR. Addition of stress-CTP with qualitative evaluation to rest-cCTA showed sensitivity, specificity, negative and positive predictive values, and accuracy at a vessel and patient level of 92%, 92%, 97%, 82%, 92% and 98%, 80%, 97%, 82%, 89%, respectively indicating a significant improvement of specificity, positive predictive value, and accuracy values vs. rest-cCTA in both models. Similarly, addition of stress-CTP with TPR evaluation to rest-cCTA showed sensitivity, specificity, negative and positive predictive values, and accuracy at a vessel and patient level of 84%, 90%, 93%, 76%, 88% and 91%, 71%, 89%, 75%, 81%, respectively indicating a significant improvement of specificity, positive predictive value values vs. rest-cCTA only in a vessel-based model and of positive predictive value in a patient-based model. When cCTA + stress-CTP with qualitative evaluation was compared with cCTA + stress-CTP with TPR estimation, no differences were found in terms of diagnostic performance.

Conclusion

The addition of stress-CTP with visual evaluation to cCTA imaging has similar diagnostic performance when compared with the quantitative analysis of myocardial perfusion based on TPR measurement.

Keywords

coronary artery disease • myocardial perfusion • computed tomography • computed tomography perfusion • accuracy • transmural perfusion ratio

* Corresponding author. Tel: +39 02 58002574; Fax: +39 02 58002231. E-mail: gianluca.pontone@ccfm.it

Published on behalf of the European Society of Cardiology. All rights reserved. © The Author(s) 2018. For permissions, please email: journals.permissions@oup.com.

Introduction

Coronary computed tomography angiography (cCTA) is a reliable imaging modality to rule out coronary artery disease (CAD)¹ with low radiation exposure² and the capability of improving prognostic assessment.³ However, despite growing acceptance in clinical practice, data are still conflicting regarding coronary anatomy evaluation with cCTA when compared with functional testing.^{4,5} This is mainly due to the limited positive predictive value of cCTA, particularly in the presence of calcified coronary lesions⁶ and lack of functional information that are frequently responsible for CAD overestimation⁷ leading to further testing with repeated ionizing radiation exposure, additional costs and CAD overtreatment.⁸

To improve the specificity and positive predictive value of cCTA, static stress computed tomography myocardial perfusion (CTP) has been recently introduced to combine anatomy and functional evaluation by a single diagnostic step.^{9,10}

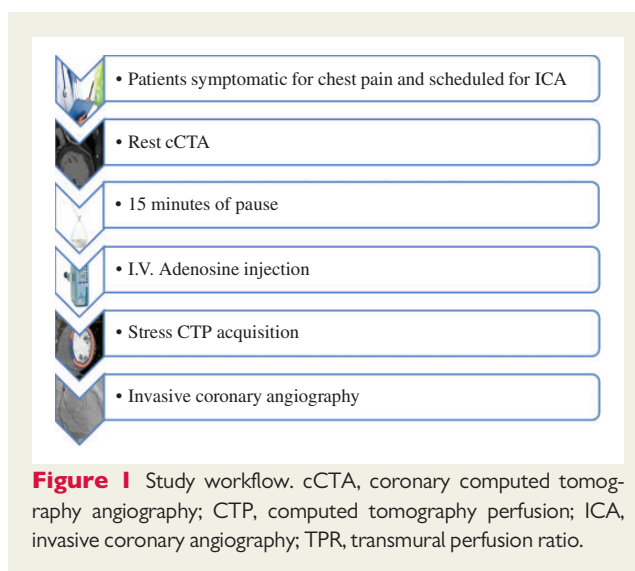
To provide a quantitative evaluation of myocardial perfusion under stress condition, several studies assessed and validated the transmural perfusion ratio (TPR) defined as the ratio of mean subendocardial attenuation to mean subepicardial attenuation,^{11–14} and they identified a TPR < 0.9 as the best threshold to define a significant myocardial perfusion defect.¹⁴ However, they used an old scanner technology (64-slice scanners), enrolled a small number of patients and employed inadequate techniques as reference standard. Recently, a last generation scanner that allows a single beat acquisition has been introduced. Therefore, in the era of new-generation scanners, there is debate on which of the two approaches (qualitative with visual evaluation or quantitative with TPR estimation) should be recommended for static stress-CTP. Therefore, aim of this study was to compare the diagnostic accuracy to detect functionally significant CAD of stress-CTP with visual approach vs. TPR quantification with a newer-generation whole-heart coverage CT scanner in consecutive symptomatic patients at intermediate-to-high risk for CAD using invasive coronary angiography (ICA) and fractional flow reserve (FFR) as reference standard.

Methods

Figure 1 shows the study protocol. Eighty-eight consecutive symptomatic patients (mean age: 66 ± 9 years, men: 63%) scheduled for ICA between October 2015 and January 2017 were prospectively enrolled. Exclusion criteria included: (i) low pre-test likelihood of CAD according to the updated Diamond-Forrester risk model¹⁵; (ii) previous history of revascularization or MI; (iii) acute presentation; (iv) contraindication to cCTA; and (v) contraindication to nitrates, β -blockade and/or adenosine. The institutional ethics committee approved the study protocol and all patients signed informed consent.

Rest-cCTA and stress-cCTA

We performed rest-cCTA with a Revolution CT Scanner (GE Healthcare, Milwaukee, WI, USA). This scanner combines 16-cm wide coverage, 0.23-mm spatial resolution thanks to Gemstone detector, faster gantry rotation time (0.28 s), intra-cycle motion-correction algorithm for temporal resolution improvement and last-generation iterative reconstruction. The acquisition was performed according to the recommendations of the Society of Cardiovascular Computed Tomography



(SCCT)¹⁶ as previously described¹⁰. After 15 min, vasodilatation was induced with i.v. adenosine injection (0.14 mg/kg/min within 4 min). At the end of the third minute of adenosine infusion, a single cCTA data sample was acquired during first-pass enhancement with the same protocol described for rest-cCTA.

Evaluation of coronary arteries in rest dataset

Rest dataset was transferred to an image-processing workstation (Advantage Workstation Version 4.7, GE Healthcare, Milwaukee, WI, USA) for analysis. The reconstructed images were evaluated in a random sequence by two cardiac imagers blinded to patient clinical history. A third cardiac imager adjudicated the scores in case of disagreement. The analysis was performed according to the SCCT guidelines for reporting.¹⁶ The coronary arteries were segmented as suggested by the American Heart Association.¹⁷ In the presence of artefacts, the best cardiac phase dataset was reconstructed using the intra-cycle motion correction algorithm.¹⁸ In each coronary artery, atherosclerosis was defined as the presence of any tissue structure larger than 1 mm² either within the coronary artery lumen or adjacent to it that was discriminated from the surrounding pericardial tissue, epicardial fat, or vessel lumen itself. The severity of coronary lesions was quantified in multi-planar curved reformatted images and categorized as none (0% luminal stenosis), very mild (1–29% luminal stenosis), mild (30–50% luminal stenosis), moderate (51% to 70% luminal stenosis), severe (71–90% luminal stenosis), sub-occluded (91–99% luminal stenosis), occluded (100% luminal stenosis), or non-evaluable. A stenosis >50% was considered obstructive from an anatomical point of view. A further secondary analysis was performed considering a stenosis > 70% obstructive at CCTA level.

Stress-CTP qualitative evaluation

Stress-CTP dataset was transferred to an image processing workstation (Advantage Workstation Version 4.7; GE Healthcare, Milwaukee, WI, USA). Myocardial segments were correlated to epicardial coronary artery territories and evaluated on short-axis (apical, mid, and basal slices) and long-axis views (2-, 3-, and 4-chamber projections) with 4–8 mm thick average multi-planar reformatted images.¹⁹ Narrow window width

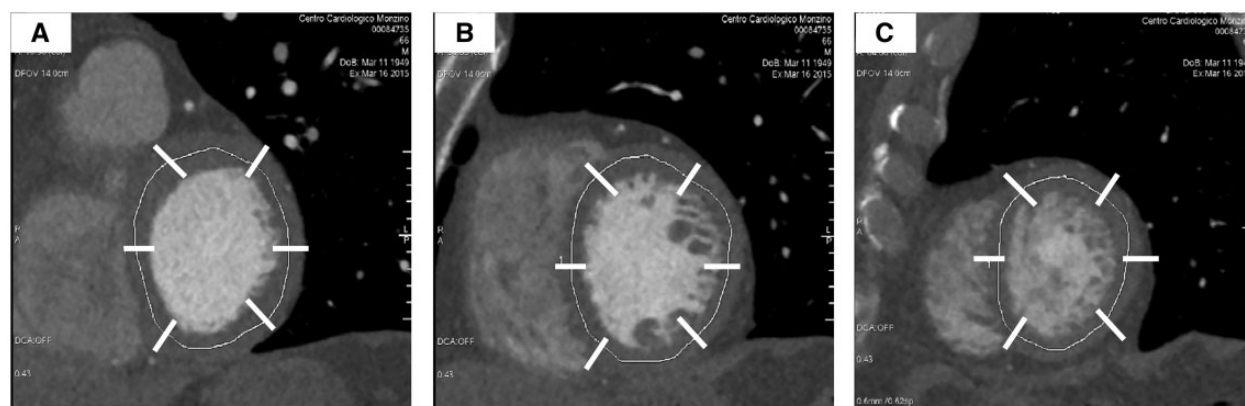


Figure 2 TPR evaluation. Static perfusion images were manually and circumferentially divided in two layers of the same thickness to define subendocardium and subepicardium at basal (A), middle (B), and apical (C) myocardial level. TPR was calculated as the ratio of subendocardium mean density to subepicardium mean density according to the ACC/AHA myocardial segmentation. TPR, transmural perfusion ratio.

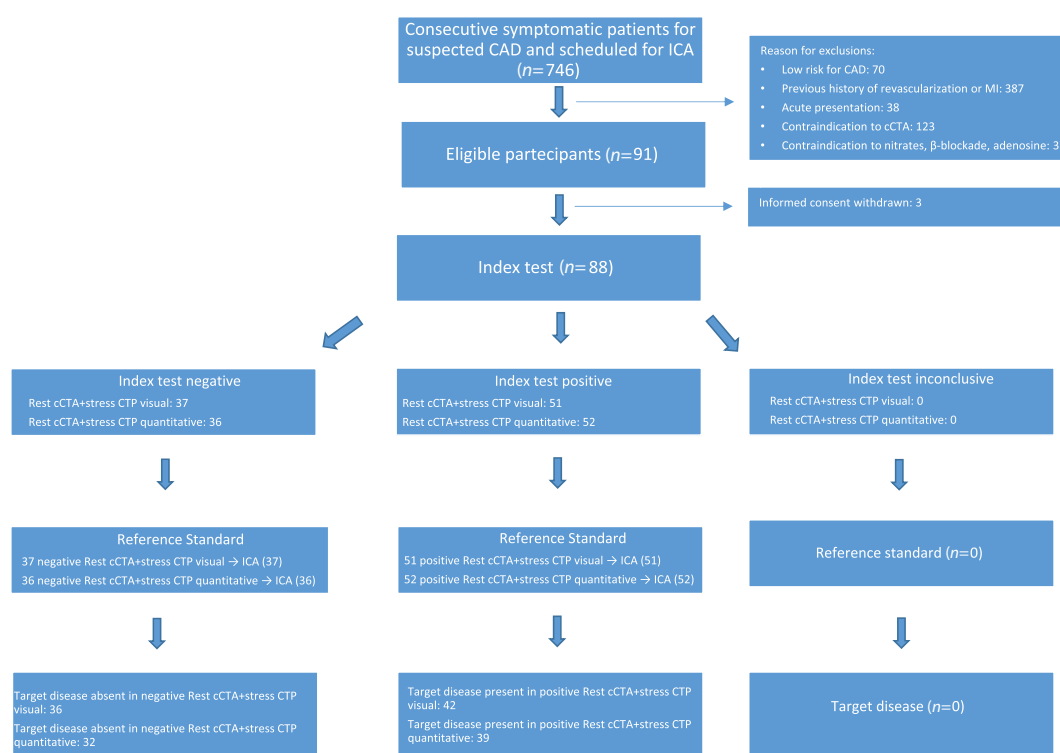


Figure 3 STARD diagram. Diagram reporting the flow of participants through the study. CAD, coronary artery disease; cCTA, coronary computed tomography angiography; CTP, computed tomography perfusion; ICA, invasive coronary angiography.

and level (350 W and 150 L, respectively) were used for perfusion defect evaluation.¹² True perfusion defects were defined as subendocardial hypoenhancements encompassing $\geq 25\%$ of the transmural myocardial thickness within a specific coronary territory.¹²

Stress-CTP quantitative evaluation

A quantitative analysis was performed to measure the TPR as previously described¹² (Figure 2). All perfusion images were divided manually and circumferentially in two layers of same thickness to define subendocardium

Table 1 Characteristics of the study population

Baseline characteristics	
Number (n)	88
Age (years), mean \pm SD	66 \pm 9
Men, n (%)	55 (62)
BMI (kg/m ²), mean \pm SD	27 \pm 4
Risk factors, n (%)	
Hypertension	68 (77)
Smoking	24 (27)
Hyperlipidaemia	59 (67)
Diabetes	15 (17)
Family history	52 (88)
Symptoms, n (%)	
Typical angina	57 (65)
Atypical angina	31 (35)
Pre-test likelihood of CAD, mean \pm SD	68 \pm 11
Reasons for invasive coronary angiography, n (%)	
Symptoms	25 (28)
Positive exercise-EKG	32 (36)
Positive stress echocardiography	5 (6)
Positive single photon emission tomography	23 (26)
Positive stress cardiac magnetic resonance	3 (3)
cCTA scan protocol, REST	
HR before scanning (bpm), mean \pm SD	68 \pm 12
β -Blocker, n (%)	44 (50)
β -Blocker dosage (mg), mean \pm SD	5.4 \pm 6.6
HR during scanning (bpm), mean \pm SD	63 \pm 9
Dose length product (mGy \cdot cm), mean \pm SD	203.4 \pm 105.2
Effective dose (mSv), mean \pm SD	2.9 \pm 1.5
cCTA scan protocol, STRESS	
HR during scanning (bpm), mean \pm SD	76.4 \pm 14
Dose length product (mGy \cdot cm), mean \pm SD	183.5 \pm 77.7
Effective dose (mSv), mean \pm SD	2.6 \pm 1.1
Prevalence of obstructive CAD (\geq 50%) at ICA, n (%)	
No disease	26 (29)
One-vessel disease	33 (38)
Two-vessel disease	14 (16)
Three-vessel disease	15 (17)
Prevalence of functionally significant CAD ^a , n (%)	43 (48)

CAD, coronary artery disease; cCTA, coronary computed tomography angiography; Ex-ECG, exercise ECG stress test; HR, heart rate; ICA, invasive coronary angiography.

^aStenosis $>$ 80% or FFR $<$ 0.8 in intermediate stenosis 30–80%.

and subepicardium. For all TPR measurements, endocardial and epicardial contours were traced, excluding papillary muscles. Then, AHA myocardial segmentation was done and mean myocardial density in Hounsfield units (HU) was measured in both layers to calculate TPR in each segment (TPR = subendocardium mean density/subepicardium mean density). Mean TPR was measured at rest and stress phase. The segmental TPR values were assigned to the respective coronary territories. Each patient was defined positive for myocardial ischaemia when TPR was $<$ 0.9 on stress-CTP and worsened when compared with rest-CTP in more than one myocardial segment.¹⁴

Adjudication selection algorithm to associate coronary arteries with myocardial segment

Blinded adjudication was performed as previously described.¹⁹ Briefly, the entry criterion for the algorithm was the presence of both at least one coronary arterial lesion of \geq 50% diameter stenosis and at least one myocardial perfusion defect. For each vessel, the following territories were identified: (i) primary territory—myocardial territories in which blood flow is supplied by the coronary vessel in the most common right dominant anatomic coronary pattern; (ii) secondary territories—myocardial territories for which blood flow may be supplied by the coronary vessel under some normal anatomic variations that need confirmation; and (iii) tertiary territories—myocardial territories where blood flow is usually not supplied by the coronary vessel.

Evaluation of coronary artery imaging combined with stress-CTP

Coronary artery imaging dataset was combined with stress-CTP according to the following interpretation: (i) non-obstructive CAD was considered negative regardless of stress-CTP findings; (ii) obstructive CAD with negative matched stress-CTP was considered negative; and (iii) obstructive CAD with positive matched stress-CTP was deemed positive.

ICA and invasive FFR performance and interpretation

Certified interventional cardiologists performed all diagnostic ICA following clinical indications and imaging standards acquisition. The coronary arteries were reported using the American Heart Association Classification system.¹⁷ Coronary angiograms were analysed with quantitative coronary angiography (QCA) (QantCor QCA; Pie Medical Imaging, Maastricht, the Netherlands) by an interventional cardiologist with more than 20 years of clinical experience in ICA performance and analysis who was blinded to the clinical history of patients and cCTA and CTP findings. All stenoses ranging between 30% and 80% were evaluated by invasive FFR.²⁰ For FFR, the pressure wire (Certus Pressure Wire, St. Jude Medical Systems, St. Paul, MI, USA) was calibrated and electronically equalized with the aortic pressure before being placed distal to the stenosis in the distal third of the coronary artery being interrogated. Glyceryl trinitrate (100 mg) was injected intracoronary to prevent vasospasm. Intravenous adenosine (140 mg/kg/min) was administered and, when steady-state hyperaemia was achieved, FFR was assessed with the RadiAnalyzer Xpress (Radi Medical Systems, Uppsala, Sweden) and calculated dividing the mean coronary pressure, measured with the pressure sensor placed distal to the stenosis, by the mean aortic pressure measured through the guide catheter. All stenosis \geq 50% were considered significant from an anatomical point of view. All stenoses \geq 80% or total occlusion or stenosis $<$ 80% but with invasive FFR \leq 0.8 were considered significant from a functional point of view.

Radiation exposure

For each patient undergoing cCTA, the effective radiation dose (ED) was calculated as the product between dose length product and a conversion coefficient for the chest ($K = 0.014$ mSv/mGy \cdot cm)²¹

Statistical analysis

Statistical analysis was performed with a dedicated software SPSS version 22.0 (SPSS, Chicago, IL, USA). Results were reported in accordance with the STARD criteria.²² Continuous variables were expressed as mean \pm standard deviation, and discrete variables were expressed as absolute numbers and percentages. The first step assessed overall evaluability

Table 2 Comparison of diagnostic accuracy between cCTA (threshold $\geq 50\%$ coronary stenoses), cCTA + stress-CTP with visual evaluation and cCTA + stress-CTP with TPR evaluation for detecting functionally significant CAD^a

	Rest cCTA	Rest-cCTA + stress-CTP visual	Rest-cCTA + stress-CTP quantitative	P-value Rest-cCTA + stress-CTP visual vs. Rest-cCTA	P-value Rest-cCTA + stress-CTP quantitative vs. Rest-cCTA	P-value Rest-cCTA + stress-CTP visual vs. Rest-cCTA + stress-CTP quantitative
Vessel-based analysis						
True positive	72	67	61			
True negative	144	176	172			
False positive	47	15	19			
False negative	1	6	12			
Sensitivity	99 (96–100)	92 (86–98)	84 (74–93)	0.004	0.062	1.000
Specificity	75 (69–82)	92 (88–96)	90 (85–95)	<0.001	<0.001	1.000
Negative predictive value	99 (98–100)	97 (94–99)	93 (89–98)	0.317	0.021	0.461
Positive predictive value	61 (50–71)	82 (72–91)	76 (65–88)	0.004	0.062	1.000
Accuracy	82 (77–87)	92 (89–96)	88 (84–93)	0.001	0.114	0.432
Patient-based analysis						
True positive	42	42	39			
True negative	23	36	32			
False positive	22	9	13			
False negative	1	1	4			
Sensitivity	98 (93–100)	98 (93–100)	91 (82–99)	1.000	0.501	0.501
Specificity	51 (37–66)	80 (68–92)	71 (58–84)	0.012	0.155	0.980
Negative predictive value	96 (88–100)	97 (92–100)	89 (79–99)	1.000	1.000	0.465
Positive predictive value	66 (54–77)	82 (72–93)	75 (63–87)	<0.001	0.009	0.501
Accuracy	74 (65–83)	89 (82–95)	81 (72–89)	0.036	0.841	0.429

All data are expressed as absolute numbers and (%) (95% CI).

cCTA, coronary computed tomography angiography; CI, confidence interval; CTP, computed tomography perfusion; FFR, fractional flow reserve; TPR, transmural perfusion ratio.

^aStenosis $>80\%$ diameter reduction or FFR <0.8 in intermediate stenosis (30–80% diameter reduction).

Red P-values indicate statistical significance.

(number of coronary segments evaluable divided by the total number of coronary segments) and sensitivity, specificity, negative and positive predictive values, and accuracy of rest-cCTA in a vessel-based and patient-based analysis. The coronary artery segments classified as non-evaluable were censored as positive. The second step assessed the diagnostic accuracy of the combined evaluation of rest-cCTA + stress-CTP with qualitative evaluation and TPR evaluation to detect functionally significant CAD in a vessel-based and patient-based model. The outcome was the presence of functionally significant CAD as detected by the combination of ICA plus invasive FFR. A true positive patient was considered in the presence of myocardial perfusion defect with matched obstructive CAD at cCTA and corresponding functionally significant CAD at invasive evaluation in agreement with pre-specified definition. A true negative patients was considered in the presence of non-obstructive CAD regardless the presence of perfusion defect and absence of functionally significant CAD at invasive evaluation in agreement with pre-specified definition.

McNemar test for dependent proportions with Bonferroni correction for multiple comparison was performed to assess differences in sensitivity, specificity, negative predictive value, positive predictive value, and accuracy. In the vessel-level analysis to account for clustered data in the same patient, the ratio estimator was used to adjust the 95% confidence interval. A P-value <0.05 was considered statistically significant.

Results

The baseline characteristics of the study population are listed in Table 1 and the study flow diagram of patients is described in Figure 3 according to STARD criteria²². The mean pre-test likelihood of obstructive CAD was $68 \pm 11\%$. All patients underwent ICA showing no CAD or negligible CAD and obstructive CAD in 158 vessels and 106 vessels, respectively. Among vessels with obstructive CAD, 32 vessels showed stenosis $\geq 80\%$ or total occlusion and 74 out of 106 vessels showed moderate stenosis, and therefore, were further evaluated by invasive FFR with the evidence of 56 vessels with no pathologic value (median 0.9, range 0.81–1.0) and 18 vessels with pathological value (median 0.71, range 0.42–0.79).

The prevalence of obstructive CAD and functionally significant CAD were 71% and 48%, respectively.

Rest-cCTA and stress-CTP were successfully performed in all patients with no side effects related to adenosine injection. Forty-four (50%) patients received metoprolol before the rest scan with an average dose of 5.4 ± 6.6 mg reaching a HR during the scan of 63 ± 9 bpm, while the mean HR during the stress scan was 76 ± 14 bpm.

Table 3 Comparison of diagnostic accuracy between cCTA (threshold $\geq 70\%$ coronary stenoses), cCTA + stress-CTP with visual evaluation and cCTA + stress-CTP with TPR evaluation for detecting functionally significant CAD^a

	Rest cCTA	Rest-cCTA + stress-CTP visual	Rest-cCTA + stress-CTP quantitative	P-value Rest-cCTA + stress-CTP visual vs. Rest-cCTA	P-value Rest-cCTA + stress-CTP quantitative vs. Rest-cCTA	P-value Rest-cCTA + stress-CTP visual vs. Rest-cCTA + stress-CTP quantitative
Vessel-based analysis						
True positive	60	58	54			
True negative	172	185	184			
False positive	19	6	7			
False negative	13	15	19			
Sensitivity	82 (74–91)	79 (71–88)	74 (64–84)	0.730	0.230	0.433
Specificity	90 (85–95)	97 (94–99)	96 (94–99)	0.007	0.014	0.777
Negative predictive value	93 (89–97)	93 (89–96)	91 (86–95)	0.858	0.404	0.501
Positive predictive value	76 (65–87)	91 (83–98)	89 (80–97)	0.021	0.050	0.701
Accuracy	88 (84–92)	92 (89–95)	90 (86–94)	0.111	0.403	0.445
Patient-based analysis						
True positive	38	37	36			
True negative	37	42	40			
False positive	8	3	5			
False negative	5	6	7			
Sensitivity	88 (79–98)	86 (76–96)	84 (73–95)	0.746	0.533	0.763
Specificity	82 (71–93)	93 (86–100)	89 (80–98)	0.179	0.368	0.458
Negative predictive value	88 (78–98)	88 (78–97)	85 (75–95)	0.931	0.680	0.734
Positive predictive value	83 (72–94)	93 (84–100)	88 (78–98)	0.170	0.497	0.478
Accuracy	85 (78–93)	90 (83–96)	86 (79–94)	0.361	0.829	0.485

All data are expressed as absolute numbers and (%) (95% CI).

cCTA, coronary computed tomography angiography; CI, confidence interval; CTP, computed tomography perfusion; FFR, fractional flow reserve; TPR, transmural perfusion ratio.

^aStenosis $>80\%$ diameter reduction or FFR <0.8 in intermediate stenosis (30–80% diameter reduction).

Red P-values indicate statistical significance.

The vessel-level sensitivity, specificity, negative and positive predictive values, and accuracy of rest-cCTA when compared with ICA and invasive FFR are listed in Table 2.

The addition of stress-CTP with qualitative evaluation to rest-cCTA provided a significant improvement of specificity, positive predictive value, and accuracy values vs. cCTA alone (Table 2) in both vessel and patient-based models.

The addition of stress-CTP with TPR evaluation to rest-cCTA showed only a significant enhancement of specificity and positive predictive value in a vessel and patient-based model, respectively, while no significant difference was found in terms of diagnostic accuracy (Table 2). Finally, when cCTA + stress CTP with qualitative evaluation was compared with cCTA + stress-CTP with TPR estimation for detecting functionally significant CAD, no differences were found in terms of diagnostic performance (Table 2). Also when a higher threshold ($>70\%$ coronary artery stenosis) was used to define a cCTA positive, the addition of stress CTP still provide significant improvement of specificity and positive predictive value in a vessel-based model (Table 3).

The mean dose-length product and ED of rest-cCTA and stress-CTP were 203.40 ± 105.14 mGy·cm and 2.8 ± 1.5 mSv and 183.5 ± 77.7 mGy·cm and 2.6 ± 1.1 mSv, respectively. The mean

time for performing the quantitative analysis was significantly longer as compared with the qualitative analysis (35 ± 6 min vs. 5 ± 2 min, $P < 0.01$). Representative case example of combined rest-cCTA and stress-cCTP with the two approaches is showed in Figure 4.

Discussion

Our main findings are that cCTA + CTP with either qualitative or quantitative evaluation has good accuracy for detecting functionally significant CAD. Moreover, both protocols improve the diagnostic performance of cCTA alone. However, TPR evaluation is associated with a trend towards lower specificity, positive predictive, and diagnostic accuracy when compared with cCTA + CTP with qualitative evaluation and is more time consuming. Thus, a protocol integrating anatomy and functional assessment using the latest-generation scanner is feasible, and provides fast and simple qualitative evaluation of myocardial perfusion allowing reliable detection of functionally significant CAD.

Previous studies validated the diagnostic accuracy of TPR in static stress-CTP.^{11–14} George et al. showed sensitivity, specificity, positive predictive and negative predictive values of the combination of cCTA

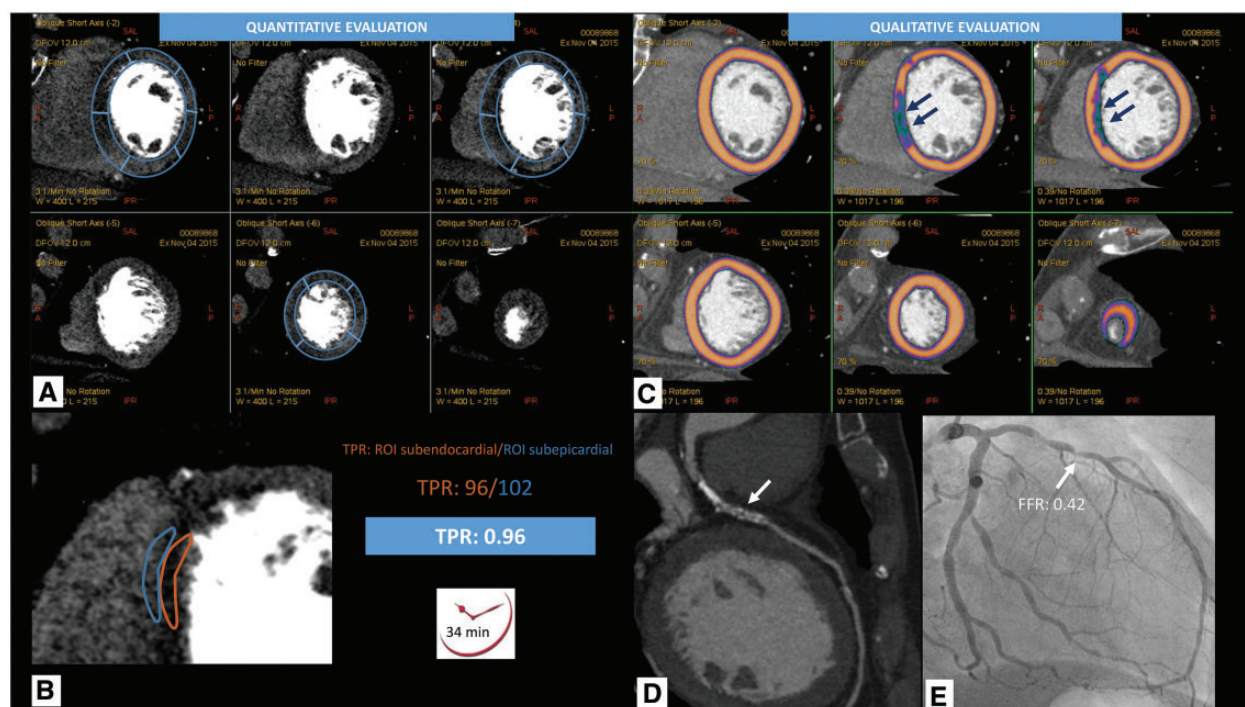


Figure 4 Comparison between qualitative and quantitative evaluation of stress-CTP. The case example demonstrates that TPR underestimates the presence of a perfusion defect due to transmural ischaemia causing pseudonormalization of mean TPR value. A 67-year-old patient with typical chest pain scheduled for ICA due to positive exercise ECG-test was evaluated with cCTA plus stress CTP. (A) Multiple short-axis views from the basis to the apex of the left ventricle. Quantitative evaluation starts with segmentation of the left ventricle (blue lines) followed by TPR measurement in each segment. (B) Blow-up image of the anterior septum basal segment. TPR is calculated as the ratio of HU measured in subendocardium to HU measured in subepicardium included in a ROI. In this case, TPR was normal (0.96). The quantitative analysis required 34 min for the entire evaluation. (C) Automatic qualitative evaluation of myocardium during stress. A software creates a map of average attenuation values of the myocardium signal. Hypoperfused segments are highlighted in blue (arrows) and are easily recognized. (D) cCTA showed a long calcified stenosis of the proximal LAD. (E) ICA confirmed severe tandem stenoses of the proximal LAD with positive FFR. BMI, body mass index; cCTA, coronary computed tomography angiography; CTP, computed tomography perfusion; FFR, fractional flow reserve; HU, Hounsfield Unit; ICA, invasive coronary angiography; LAD, left anterior descending artery; LCX, left circumflex artery; ROI, region of interest; TPR, transmural perfusion ratio.

and CTP with TPR for the detection of obstructive coronary lesions causing perfusion abnormalities of 86%, 92%, 92%, and 85% in a per-patient analysis and of 79%, 91%, 75%, and 92% in a per-vessel/territory analysis, respectively. Similarly, Cury *et al.*¹² showed a good correlation ($r = 0.74$, $P < 0.001$) between TPR and the combination of ICA plus single-photon emission computed tomography (SPECT) for detecting significant coronary disease but found a lower TPR in the ischaemic myocardium when compared with remote myocardium (0.71 ± 0.13 vs. 1.01 ± 0.09 , $P < 0.001$). Furthermore, Hosokawa *et al.*¹³ demonstrated a significant correlation between a modified version of TPR normalized for left ventricular thickness and a myocardial perfusion stress score assessed by SPECT. However, it is noteworthy that in all these studies the sample size was small, the imaging technology most frequently used was a 64-slice scanner and the reference standard was the combination of ICA + SPECT rather than the combination of ICA + FFR. More recently, George *et al.*¹⁴ showed an excellent area under the curve (AUC = 0.92) of TPR measurement to detect ischaemia using a 320-slice scanner. However, also in this study the reference standard was SPECT.

Indeed, ICA + FFR is currently considered the gold standard approach for detecting haemodynamically significant lesions, while SPECT cannot be considered the ideal tool, particularly in patients with multi-vessel ischaemia.

A potential explanation for the similar performance between qualitative versus quantitative evaluation could be related to some tips typically used in qualitative evaluation to distinguish between artefacts and true perfusion defect that are not applicable for TPR analysis. First, improved coverage in the z-axis that allows the scanner to acquire images in a single beat avoiding the different contrast attenuation from the base to apex of the myocardium, a phenomenon that usually occurs with previous generation scanners and may mimic a perfusion defect.²³ Second, the increased spatial resolution due to the integrated use of the Gemston detector and last-generation iterative reconstruction algorithm enables the cardiac imager to detect small differences in myocardial density between normal and hypoperfused myocardium that usually are about 50 HU.^{24–26} Finally, the high temporal resolution of the last-generation scanners limits the risk of misregistration caused by the usual HR increase occurring after

adenosine injection. Despite all these improvements, beam hardening is still a problem particularly with lower-energy X-rays that are used, as in our study, to reduce the overall radiation exposure.²⁷ The phenomenon is responsible for local inhomogeneity that may mimic a perfusion defect. This may affect TPR measurement by reducing its mean value and may cause false positive results. On the contrary, qualitative evaluation with a visual approach allows the cardiac imager to use several tactics for differentiating true from false perfusion defects. Indeed, the hypoenhanced region usually has a triangular shape, originates from the region of high attenuation next to it and does not conform to vascular territories.²⁷ In addition, the typical location of hypoenhancement is the basal inferolateral wall due to its proximity to the contrast-filled descending aorta and high-density vertebral bodies.²⁷ Finally, with multi-phase acquisition the true perfusion defect persists, while the artefact disappears or more commonly changes its location.²⁷ Use of these strategies is possible with the visual approach only and may overcome the difficulty of clearly differentiating an artefact from a true defect, thus reducing false positive findings and achieving a better performance when compared with the TPR technique.

To have a quantitative analysis with static CTP, we will have to wait for the integration of dual-energy computed tomography (DECT) in the scanner.²⁸ Ko *et al.*²⁹ used DECT with adenosine stress and perfusion magnetic resonance as the reference standard and found a sensitivity, specificity, and accuracy of 89%, 78%, and 82%, respectively for the detection of myocardial segments with perfusion defects. However, as in the previous studies, the scanner they used did not have wide coverage and the reference standard was not ICA and FFR.

Some limitations of our study should be acknowledged. First, the study population of our article is at intermediate to high risk for CAD and this is not the typical target of CCTA in real clinical word.³⁰ However, CCTA alone is an already established tool to rule out significant CAD in this setting, while the true additional diagnostic value of CTP was proved in a higher risk population.¹⁰ Similarly, patients with previous history of revascularization were not included but in this setting cCTA is not still indicated for routine use. Second, invasive FFR was not performed in all vessels but only in those with intermediate stenoses. Third, when invasive FFR is used as the reference standard for detecting ischaemia, we should take in account the possibility that microvascular disease is associated with normal FFR and pathologic CTP. Third, the sample size of the study was small and therefore this study should be considered a pilot experience only. Finally, we used a rest-stress protocol that may be limited by the contamination, throughout the entire stress phase, of the contrast agent administered during the rest acquisition.

Conclusions

In conclusions, our results suggest that the addition of stress-CTP with visual evaluation in patients at intermediate-to-high risk for CAD is a feasible and more effective strategy to improve the diagnostic accuracy of cCTA imaging when compared with the quantitative analysis of myocardial perfusion based on TPR measurement.

Funding

This work was supported by the Italian Ministry of Health, Rome, Italy [Ricerca Corrente 2014-2017 BIO 19].

Conflict of interest: G.P. received institutional fee as speaker or research grant from GE Healthcare, Bracco, Medtronic, Bayer, Heartflow; A.D. received institutional fee for research grant of fee as speaker from GE Healthcare, Bracco, Heartflow.

References

1. Mark DB, Berman DS, Budoff MJ, Carr JJ, Gerber TC, Hecht HS *et al.* ACCF/ACR/AHA/NASCI/SAIP/SCAI/SCCT 2010 expert consensus document on coronary computed tomographic angiography: a report of the American College of Cardiology Foundation Task Force on Expert Consensus Documents. *Catheter Cardiovasc Interv* 2010;**76**:E1–42.
2. Pontone G, Andreini D, Bartorelli AL, Cortinovis S, Mushtaq S, Bertella E *et al.* Diagnostic accuracy of coronary computed tomography angiography: a comparison between prospective and retrospective electrocardiogram triggering. *J Am Coll Cardiol* 2009;**54**:346–55.
3. Pontone G, Andreini D, Bartorelli AL, Bertella E, Cortinovis S, Mushtaq S *et al.* A long-term prognostic value of CT angiography and exercise ECG in patients with suspected CAD. *JACC Cardiovasc Imaging* 2013;**6**:641–50.
4. Douglas PS, Hoffmann U, Patel MR, Mark DB, Al-Khalidi HR, Cavanaugh B *et al.* Outcomes of anatomical versus functional testing for coronary artery disease. *N Engl J Med* 2015;**372**:1291–300.
5. Investigators S-H. CT coronary angiography in patients with suspected angina due to coronary heart disease (SCOT-HEART): an open-label, parallel-group, multicentre trial. *Lancet* 2015;**385**:2383–91.
6. Pontone G, Bertella E, Mushtaq S, Loguercio M, Cortinovis S, Baggiano A *et al.* Coronary artery disease: diagnostic accuracy of CT coronary angiography—a comparison of high and standard spatial resolution scanning. *Radiology* 2014;**271**:688–94.
7. Mowatt G, Cook JA, Hillis GS, Walker S, Fraser C, Jia X *et al.* 64-Slice computed tomography angiography in the diagnosis and assessment of coronary artery disease: systematic review and meta-analysis. *Heart* 2008;**94**:1386–93.
8. Pontone G, Andreini D, Guaricci AI, Rota C, Guglielmo M, Mushtaq S *et al.* The STRATEGY study (Stress Cardiac Magnetic Resonance Versus Computed Tomography Coronary Angiography for the Management of Symptomatic Revascularized Patients): resources and outcomes impact. *Circ Cardiovasc Imaging* 2016;**9**:e005171.
9. Rossi A, Merkus D, Klotz E, Mollet N, de Feyter PJ, Krestin GP. Stress myocardial perfusion: imaging with multidetector CT. *Radiology* 2014;**270**:25–46.
10. Pontone G, Andreini D, Guaricci AI, Baggiano A, Fazzari F, Guglielmo M *et al.* Incremental diagnostic value of stress computed tomography myocardial perfusion with whole-heart coverage CT scanner in intermediate to high-risk symptomatic patients suspected of coronary artery disease. *JACC Cardiovasc Imaging* 2018; doi:10.1016/j.jcmg.2017.10.025.
11. George RT, Arbab-Zadeh A, Miller JM, Kitagawa K, Chang HJ, Bluemke DA *et al.* Adenosine stress 64- and 256-row detector computed tomography angiography and perfusion imaging: a pilot study evaluating the transmural extent of perfusion abnormalities to predict atherosclerosis causing myocardial ischemia. *Circ Cardiovasc Imaging* 2009;**2**:174–82.
12. Cury RC, Magalhaes TA, Paladino AT, Shiozaki AA, Perini M, Senra T *et al.* Dipyridamole stress and rest transmural myocardial perfusion ratio evaluation by 64 detector-row computed tomography. *J Cardiovasc Comput Tomogr* 2011;**5**:443–8.
13. Hosokawa K, Kurata A, Kido T, Shikata F, Imagawa H, Kawachi K *et al.* Transmural perfusion gradient in adenosine triphosphate stress myocardial perfusion computed tomography. *Circ J* 2011;**75**:1905–12.
14. George RT, Arbab-Zadeh A, Miller JM, Vavere AL, Bengel FM, Lardo AC *et al.* Computed tomography myocardial perfusion imaging with 320-row detector computed tomography accurately detects myocardial ischemia in patients with obstructive coronary artery disease. *Circ Cardiovasc Imaging* 2012;**5**:333–40.
15. Genders TS, Steyerberg EW, Alkadhi H, Leschka S, Desbiolles L, Nieman K *et al.* A clinical prediction rule for the diagnosis of coronary artery disease: validation, updating, and extension. *Eur Heart J* 2011;**32**:1316–30.
16. Leipsic J, Abbata S, Achenbach S, Cury R, Earls JP, Mancini GJ *et al.* SCCT guidelines for the interpretation and reporting of coronary CT angiography: a report of the Society of Cardiovascular Computed Tomography Guidelines Committee. *J Cardiovasc Comput Tomogr* 2014;**8**:342–58.
17. Austen WG, Edwards JE, Frye RL, Gensini GG, Gott VL, Griffith LS *et al.* A reporting system on patients evaluated for coronary artery disease. Report of the Ad Hoc Committee for Grading of Coronary Artery Disease, Council on Cardiovascular Surgery, American Heart Association. *Circulation* 1975;**51**:5–40.

18. Pontone G, Andreini D, Bertella E, Baggiano A, Mushtaq S, Loguercio M *et al.* Impact of an intra-cycle motion correction algorithm on overall evaluability and diagnostic accuracy of computed tomography coronary angiography. *Eur Radiol* 2016;**26**:147–56.
19. Cerci RJ, Arbab-Zadeh A, George RT, Miller JM, Vavere AL, Mehra V *et al.* Aligning coronary anatomy and myocardial perfusion territories: an algorithm for the CORE320 multicenter study. *Circ Cardiovasc Imaging* 2012;**5**:587–95.
20. De Bruyne B, Pijls NH, Kalesan B, Barbato E, Tonino PA, Piroth Z *et al.* Fractional flow reserve-guided PCI versus medical therapy in stable coronary disease. *N Engl J Med* 2012;**367**:991–1001.
21. Einstein AJ, Moser KW, Thompson RC, Cerqueira MD, Henzlova MJ. Radiation dose to patients from cardiac diagnostic imaging. *Circulation* 2007;**116**:1290–305.
22. Bossuyt PM, Reitsma JB, Bruns DE, Gatsonis CA, Glasziou PP, Irwig L *et al.* STARD 2015: an updated list of essential items for reporting diagnostic accuracy studies. *Radiology* 2015;**277**:826–32.
23. Rossi A, Dharampal A, Wragg A, Davies LC, van Geuns RJ, Anagnostopoulos C *et al.* Diagnostic performance of hyperaemic myocardial blood flow index obtained by dynamic computed tomography: does it predict functionally significant coronary lesions? *Eur Heart J Cardiovasc Imaging* 2014;**15**:85–94.
24. George RT, Arbab-Zadeh A, Cerci RJ, Vavere AL, Kitagawa K, Dewey M *et al.* Diagnostic performance of combined noninvasive coronary angiography and myocardial perfusion imaging using 320-MDCT: the CT angiography and perfusion methods of the CORE320 multicenter multinational diagnostic study. *AJR Am J Roentgenol* 2011;**197**:829–37.
25. George RT, Jerosch-Herold M, Silva C, Kitagawa K, Bluemke DA, Lima JA *et al.* Quantification of myocardial perfusion using dynamic 64-detector computed tomography. *Invest Radiol* 2007;**42**:815–22.
26. George RT, Silva C, Cordeiro MA, DiPaula A, Thompson DR, McCarthy WF *et al.* Multidetector computed tomography myocardial perfusion imaging during adenosine stress. *J Am Coll Cardiol* 2006;**48**:153–60.
27. Techasith T, Cury RC. Stress myocardial CT perfusion: an update and future perspective. *JACC Cardiovasc Imaging* 2011;**4**:905–16.
28. Johnson TR, Krauss B, Sedlmair M, Grasruck M, Bruder H, Morhard D *et al.* Material differentiation by dual energy CT: initial experience. *Eur Radiol* 2007;**17**:1510–7.
29. Ko SM, Choi JW, Hwang HK, Song MG, Shin JK, Chee HK. Diagnostic performance of combined noninvasive anatomic and functional assessment with dual-source CT and adenosine-induced stress dual-energy CT for detection of significant coronary stenosis. *AJR Am J Roentgenol* 2012;**198**:512–20.
30. Montalescot G, Sechtem U, Achenbach S, Andreotti F, Arden C, Budaj A *et al.* 2013 ESC guidelines on the management of stable coronary artery disease: the Task Force on the management of stable coronary artery disease of the European Society of Cardiology. *Eur Heart J* 2013;**34**:2949–3003.